JOURNAL OF AIRCRAFT
Vol. 33, No. 4, July–August 1996

# Computational Fluid–Structure Interaction Model for Parachute Inflation

Richard John Benney* and Keith Robert Stein*
*U.S. Army Natick Research, Development, and Engineering Center, Natick, Massachusetts 01760-5017*

**In parachute research, the canopy inflation process is the least understood and the most complex to model. Unfortunately it is during the opening process that the canopy often experiences the largest deformations and loadings. The complexity of modeling the opening process stems from the coupling between the structural dynamics of the canopy, lines, and payload with the aerodynamics of the surrounding fluid medium. The addition of a computational capability to model the coupled opening behavior would greatly assist in the understanding of the canopy inflation process. This article describes research that involves coupling a computational fluid dynamics code to a mass spring damper parachute structural code. The axisymmetric codes are coupled with an explicit marching method. The current model is described and results for a round parachute are presented. A comparison of the numerical results to experimental data will be presented. The successful solution of these problems gives us confidence that the computational aeroelastic problem for parachute openings can be solved. This solution allows moving the parachute design process from one of cut and try to one based on experimentally verified computational tools and reduces the reliance on costly and time-consuming testing during development.**

## Nomenclature

CALA$x$ = $X$ direction force contribution from canopy loads analysis logic
CALA$y$ = $Y$ direction force contribution from canopy loads analysis logic
$Cm_i$ = meridional damping constant
$Cn_i$ = normal damping constant
$DX_i$ = $X$ direction force contribution from normal line drag
$DY_i$ = $Y$ direction force contribution from normal line drag
$F1$ = normal force contribution
$F2$, $F3$ = tangential force contribution
$F4$ = gravitational force contribution
$g$ = gravitational constant
$km_i$ = meridional spring constant
$P$, $Q$ = C-grid forcing functions
$m_i$ = mass associated with node $i$
$n$ = total number of nodes on canopy
$nl$ = total number of nodes on line
$t$ = time
$x$ = radial computational fluid dynamics grid coordinate
$x(i)$ = current $x$ location of node $i$
$y$ = axial computational fluid dynamics grid coordinate
$y(i)$ = current $y$ location of node $i$
$\alpha_i$ = angle defining normal direction of node $i$
$\beta_i$ = angle defining relative angle between nodes $i$ and $i + 1$
$\Delta l_i$ = positive amount of stretch between nodes $i$ and $i + 1$
$\eta$ = computational domain coordinate
$\xi$ = computational domain coordinate
$\psi$ = gore bulge angle

Received Dec. 30, 1994; revision received April 11, 1996; accepted for publication April 16, 1996. This paper is declared a work of the U.S. Government and is not subject to copyright protection in the United States.

*Aerospace Engineer, Mobility Directorate, Kansas Street. Member AIAA.

## Introduction

THE time-variant aerodynamic characteristics associated with the opening of a parachute are extremely complex to model. The complexity arises largely from the fact that the flowfield is dependent on the canopy shape, which is itself dependent on the flowfield. A correct model must include the coupled behavior of the parachute system's structural dynamics with the aerodynamics of the surrounding flowfield. A coupled model not only will provide information about the opening characteristics of a parachute, but also will provide characteristics of the parachute in its terminal velocity state, including the parachute's shape, drag, velocity, pressure distribution, and flowfield characteristics.

The aerodynamic or the structural dynamic behavior of the parachute opening problem cannot be studied independently (decoupled) with accuracy. The logic required in coupling a computational fluid dynamic (CFD) code to a structural dynamic code was established in stages of increasing complexity. The model described in this report is axisymmetric and has evolved from previous efforts.[1,2] The present model involves coupling the CFD code to a mass spring damper (MSD) structural dynamic code to represent a flat, circular solid cloth parachute. A half-scale C-9 canopy dropped from rest is modeled and the computational results will be compared with experimental results.

## CFD Model

The simplified arbitrary Lagrangian–Eulerian (SALE) Navier–Stokes code, written at Los Alamos National Laboratories, has been adapted to model parachute problems.[3] SALE uses a finite difference algorithm to solve the time-dependent, two-dimensional, Navier–Stokes equations (incompressible or compressible) in Cartesian or axisymmetric coordinates. Axisymmetric coordinates are used for parachute applications.

SALE defines velocities at cell vertices in the computational grid, whereas pressures are defined at cell centers. SALE uses the arbitrary Lagrangian–Eulerian (ALE) algorithm, which allows the use of nonuniform computational grids that can deform with time. The computational domain is discretized with a single block grid consisting of quadrilateral cells. The re-

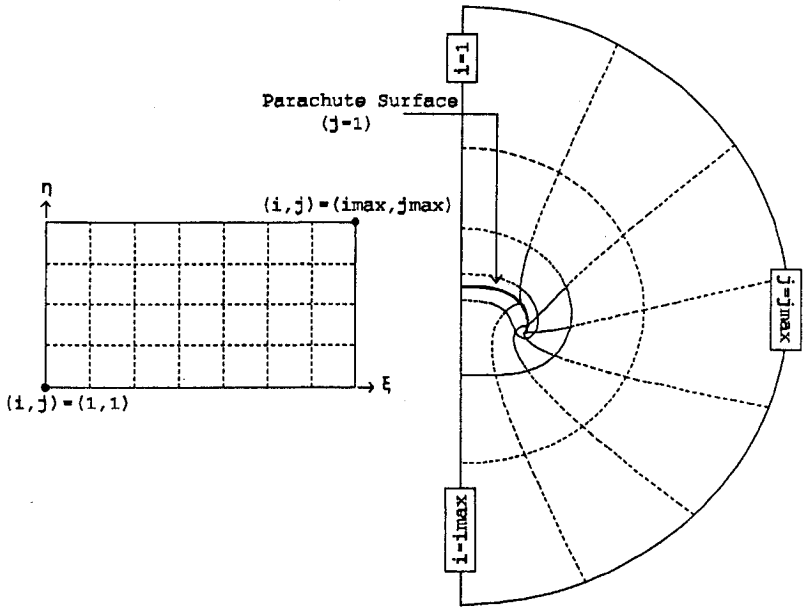


**Fig. 1 C-grid computational and physical domains.**

zoning capabilities of SALE are valuable for solving flows about decelerators in motion or for inflation problems.

Parachute inflation problems have been addressed utilizing an elliptic C-grid mesh update strategy. Much effort has been devoted to elliptic grid generation and some of the developed techniques and strategies have been incorporated into the axisymmetric parachute model. A C-grid takes a single block grid in the computational domain and maps one of its outer boundaries around the surface of a body in the physical domain. In the case of the current application, one boundary wraps around the parachute cross section (see Fig. 1). The two boundaries that border the surface boundary in the computational domain map onto the symmetry axis above and below the parachute surface boundary in the physical domain. The final boundary in the computational domain corresponds to the outer boundary in the physical domain.

The elliptic grid is generated by solving a form of the Poisson equation. A general form of Poisson's equation is shown in Eqs. (1) and (2):

$$\xi_{xx} + \xi_{yy} = P(\xi, \eta) \tag{1}$$

$$\eta_{xx} + \eta_{yy} = Q(\xi, \eta) \tag{2}$$

where $P$ and $Q$ are forcing functions that result in desired grid coordinate control.

## MSD Model

The parachute consisting of canopy, lines, and payload is modeled as a series of lumped mass points (nodes) connected by springs and dampers as shown in Fig. 2. The MSD model fits into the coupled code as a set of Fortran subroutines. The MSD subroutines require a pressure distribution along the meridional length of the canopy and a time step as input. The MSD program returns the position and velocity of each MSD canopy node and the payload node to the CFD program at the requested time.

The MSD model is axisymmetric but includes some three-dimensional considerations. The current model has been used to approximate flat, circular, solid cloth canopies, such as a C-9. The MSD governing equations are obtained by applying Newton's second law at each user-defined node to obtain a set of coupled nonlinear differential equations. A typical interior node on the canopy surface experiences four major force contributions. These forces include a normal contribution, two meridional spring and damper contributions, and a gravitational contribution. The gravitational force is the product of the gravitational acceleration constant and the mass of the node. A free body diagram of a typical interior node on the canopy surface is shown in Fig. 3. The MSD code is limited to axisymmetric problems.

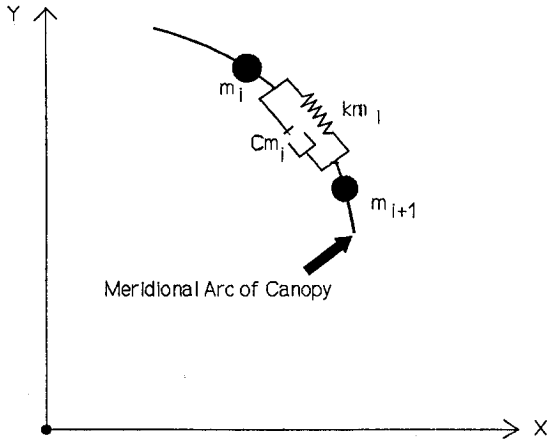


**Fig. 2 Mass spring damper model.**

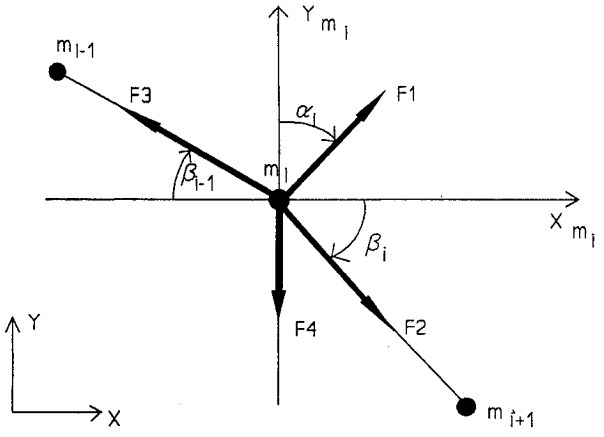


**Fig. 3 Free body diagram.**

The normal force contribution is principally because of the aerodynamic differential pressure acting across the canopy surface. The current model converts the pressure loading to localized forces at each node by using an approximation of the logic contained in the canopy loads analysis (CALA) code theory.[4] The CALA code is a static code only and predicts the steady-state shape of a parachute system, but requires a steady-state pressure distribution along a radial (meridional arc length) as input.

The pressure distribution across the surface of the canopy is supplied by the CFD code at the MSD nodes. The MSD code utilizes the basic CALA assumptions to transform the pressure distribution into nodal forces tangential and normal to the radial position. The MSD nodes are located along a radial and the mass associated with each are lumped values based on the constructed shape of the canopy gores. The CALA code assumes that the horizontal members of a gore form sections of circular arcs and that the pressure distribution is uniform along the horizontal members. The horizontal members lie in planes that are defined by the current unit normal vectors from two adjacent radials making up one gore. The CALA code[4] defines the static force per unit radial length applied to a radial location. The value of the normal and tangential forces per unit length is given in the CALA reference. These force equations include the variable $\psi$. The variable $\psi$ is used to define the circular arc section at each node point. This angle $\psi$ is determined iteratively using Newton's method at each node for each current surface configuration based on the constructed gore shape at each time step. The forces include approximations of the hoop force contribution based on the gore geometry. The CALA logic has many assumptions that need to be addressed. These include the assumed gore shape, the orientation of the normal to the canopy surface, singularities with small gore bulge angles, the snap-through phenomena (which occur when the pressure distribution changes sign), and gore-on-gore contact regions, especially during the initial stages of the opening.

The normal force on a typical canopy node also includes a variable viscous normal damping contribution. This damping is applied to the node based on the normal velocity of each canopy node relative to the payload velocity. The normal damping is included primarily to maintain numerical stability of the overall solution. The dampers are not attempting to model any physically observable phenomenon. The value used for the normal damping constant can have a major impact on the solution.[2]

The tangential force contribution to each node is the sum of the forces from the meridional springs and dampers connecting each node to its nearest neighbor. The spring force is the product of the spring constant and the change in length between nodes. The spring force acts only when the distance between the nodes is greater than the constructed distance because canopy fabric cannot support compressive forces. The tangential damping force opposes the relative velocity between neighboring nodes. The force is the product of the damping constant and the relative change in velocity between two adjacent nodes. These dampers are included to damp out the high natural frequencies in the meridional springs. These natural frequencies may cause flow instabilities in connection with the no-slip boundary conditions at the canopy surface.

The canopy and suspension lines are modeled with a user-defined number of nodes $n$ and $nl$, respectively. The payload is defined with one node. The total number of nodes is equal to $(n + nl + 1)$. The equations of motion for all canopy and line nodes have two degrees of freedom and are defined in the global $X$, $Y$ coordinate system. The payload has only one degree of freedom in the global $Y$ direction. Therefore, the MSD model is solving $(2n + 2nl + 1)$ second-order nonlinear ordinary differential equations (ODEs).

The equations of motion for interior canopy nodes (nodes 2 through $n - 1$) are described in this section. The acceleration in the $x$ direction of canopy node $i$ is given in Eq. (3):

$$\frac{d^2x(i)}{dt^2} = \frac{1}{m_i}\left(\text{CALA}x + km_i\Delta l_i \cos\beta_i - km_{i-1}\Delta l_{i-1}\cos\beta_{i-1} + Cm_i\frac{d(\Delta l_i)}{dt}\cos\beta_i - Cm_{i-1}\frac{d(\Delta l_{i-1})}{dt}\cos\beta_{i-1} - Cn_i\left\{\frac{dx(i)}{dt}\sin\alpha_i + \left[\frac{dy(i)}{dt} - \frac{dy(\text{payload})}{dt}\right]\cos\alpha_i\right\}\sin\alpha_i\right) \tag{3}$$

The acceleration in the $y$ direction of canopy node $i$ is given in Eq. (4):

$$\frac{d^2y(i)}{dt^2} = \frac{1}{m_i}\left(\text{CALA}y - km_i\Delta l_i \sin\beta_i + km_{i-1}\Delta l_{i-1}\sin\beta_{i-1} - Cm_i\frac{d(\Delta l_i)}{dt}\sin\beta_i + Cm_{i-1}\frac{d(\Delta l_{i-1})}{dt}\sin\beta_{i-1} - Cn_i\left\{\frac{dx(i)}{dt}\sin\alpha_i + \left[\frac{dy(i)}{dt} - \frac{dy(\text{payload})}{dt}\right]\cos\alpha_i\right\}\cos\alpha_i\right) - g \tag{4}$$

Next, equations for a typical interior line node are given. These include line nodes no. 2 through no. $nl - 1$. The acceleration in the $x$ direction of line node $i$ is given in Eq. (5):

$$\frac{d^2x(i)}{dt^2} = \frac{1}{m_i}\left[km_i\Delta l_i\cos\beta_i - km_{i-1}\Delta l_{i-1}\cos\beta_{i-1} + Cm_i\frac{d(\Delta l_i)}{dt}\cos\beta_i - Cm_{i-1}\frac{d(\Delta l_{i-1})}{dt}\cos\beta_{i-1} - DX_i\right] \tag{5}$$

The acceleration in the $y$ direction of line node $i$ is given in Eq. (6):

$$\frac{d^2y(i)}{dt^2} = \frac{1}{m_i}\left[-km_i\Delta l_i\sin\beta_i + km_{i-1}\Delta l_{i-1}\sin\beta_{i-1} - Cm_i\frac{d(\Delta l_i)}{dt}\sin\beta_i + Cm_{i-1}\frac{d(\Delta l_{i-1})}{dt}\sin\beta_{i-1} - DY_i\right] - g \tag{6}$$

These governing equations representing the canopy, lines, and payload are reformulated into a set of first-order ODEs that are nonlinear in space and first order in time. The ODEs are solved over the desired time step with initial conditions by utilizing the Sandia, Los Alamos, Air Force Weapons Laboratory Technical Exchange Committee (SLATEC) ODE solver DDEBDF and associated subroutines.[5] For more detail on the individual terms in Eqs. (3–6) see Ref. 2.

The initial conditions required to solve the governing ODEs are to prescribe the initial position and velocity of every node in the MSD model. Initial shapes were constructed by defining an angle from the axis of symmetry to the parachute suspension line (always assumed to be initially straight) and generating a conical base with a spherical section top where the total arc length is given by the constructed geometry. The initial velocities of all nodes must also be specified to generate a solution. The simplest case is to set all velocities equal to zero. Different initial conditions must be employed to model more accurately other types of real parachute openings.

## Coupling

The coupling approach in the parachute model is explicit in time. The CFD code is used as the main Fortran program, which calls the structural code subroutines. The coupled model starts the computations with the flow medium and structural components at rest. During each time step in the coupled run the CFD and structural dynamic computations are advanced one time step.

For each CFD time step, three tasks must be performed. First, the C-grid canopy surface is redefined each time step to correspond to the current structural shape. At each time step, the structural code returns updated positions and velocities for canopy nodes to the CFD code. These positions are used to update the canopy surface in the C-grid. The new CFD surface nodes are determined by interpolation from the structural surface nodes using Lagrange polynomials. The surface is then given a thickness normal to the interpolated positions. Secondly, the elliptic grid is updated based on the updated canopy surface representation. The elliptic grid is defined by repositioning the surface boundary, repositioning the outer boundary, and then updating interior nodes and nodes along the symmetry axis. The outer boundary moves each time step with the parachute payload. Interior grid nodes are updated with Poisson's equation and the same set of clustering coefficients that were used to generate the initial C-grid. The C-grid for the previous time step is used as the initial guess for the updated C-grid generation. Finally, appropriate boundary conditions are defined. Boundary conditions on the canopy surface are defined to represent a no-slip, nonporous surface. The outer boundary is assumed to be the far field and velocity components are defined as zero ($u = v = 0$) at the outer boundaries. The symmetry axis is given a freeslip boundary by setting the normal component of velocity $u$ to zero on the symmetry axis. After the grid is updated and boundary conditions are specified as described previously, the CFD solution is advanced one time step.

For each MSD time step, two tasks must be performed. First, the differential pressure distribution for the canopy surface is determined from the CFD solution. Since SALE computes pressures at cell centers, nodal pressure values along the canopy surface are defined as the average of the pressures in the two surrounding cells. Pressures on the axis of symmetry nodes are defined as the pressure in the adjacent corner cell. Lower and upper surface pressures are subtracted to get the differential pressure distribution for the meridional distribution of CFD surface nodes. The CFD pressure distribution is interpolated to the structural surface node distribution. Using the distribution of nodes in the structural representation, the pressures are determined by interpolation from the CFD distribution of nodes using Lagrange polynomials. Finally, the structural model uses the CFD pressure distribution to advance the structural solution one time step and updated positions are once again returned to the CFD code. The C-grid is then updated, boundary conditions are defined, and the process continues.

## Results

The coupled computer model was tested by modeling a variety of axisymmetric canopies that either are used by the U.S. Army for personnel/cargo or are scaled versions of common parachutes being used in experiments.[2] Results from one simulation will be presented and the numerical results compared to experimental results.

The coupled numerical model simulates a half-scale C-9 solid cloth canopy (14-ft constructed diameter), which is dropped from rest. The parachute system is hanging from a ceiling with a release mechanism attached to the apex. The canopy hangs from the apex, the lines hang from the skirt and the payload is hanging from the bottom of the lines. The apex connection is released at time equal to 0 s.

The simulation was run with material properties that are crude approximations of the experimental model (see Ref. 2 for more details on properties used to model this canopy). The CFD grid size is 70 by 60 cells. The number of nodes on the canopy and lines are 25 and 15, respectively. The numbers used were chosen by experience with consideration given to obtaining results in an acceptable period of time. The payload weight is 42.5 lb. The unstretched line length is 12 ft and the C-9 canopy is constructed from 28 gores. The simulation was

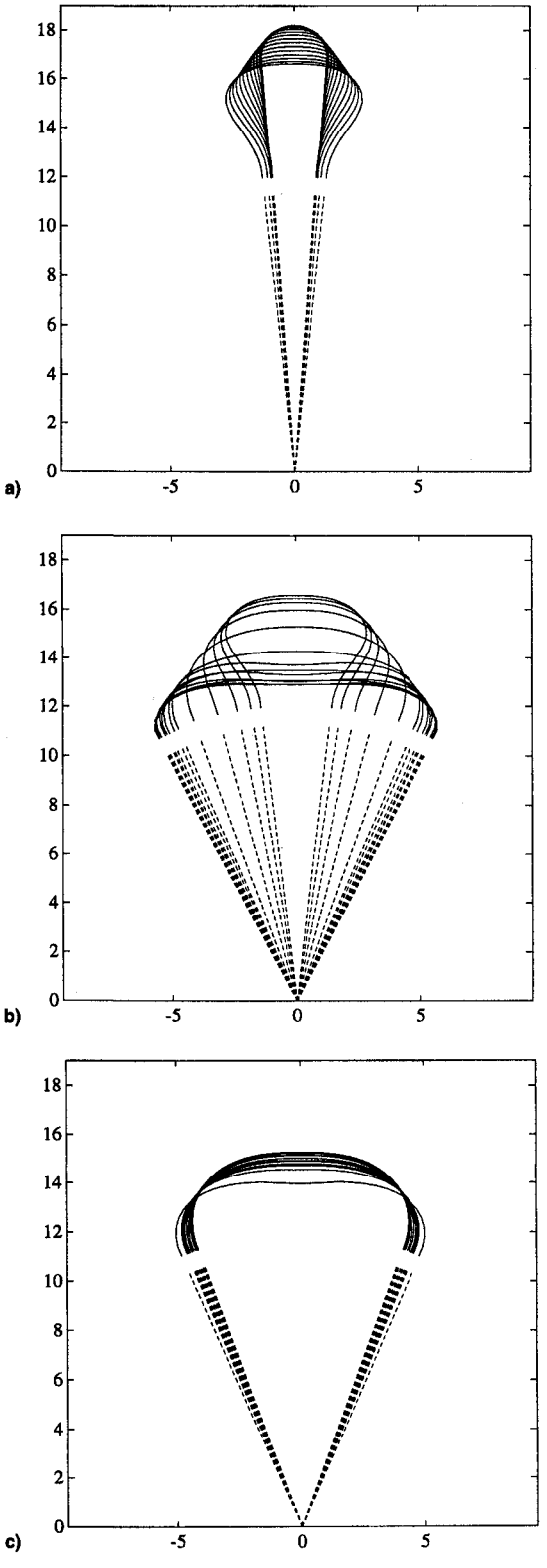


**Fig. 4 Canopy shape vs time (axes in feet): a) $0.0 < t < 1.0$, b) $1.0 < t < 2.0$, and c) $2.0 < t < 3.0$ s.**

run on a Kubota Titan 3000 minisupercomputer (U.S. Army supercomputers have also been utilized). The time step for the run was $3 \times 10^{-6}$ s, determined by experience with the coupled codes to maintain numerical stability throughout the computation. The coupled codes have not been optimized for performance. Optimization and programming for specific high-speed machine capabilities will be addressed for the next-generation coupled codes.

The origin is user defined and was chosen for this run to coincide with the initial location of the payload node point. Figure 4a shows a sequence of canopy shapes from a fixed payload reference for equally spaced time steps from the initial unstretched shape at time equal to 0.0 s up to time equal to 1.0 s. Figures 4b and 4c are a continuation of Fig. 4a for times from 1.0 to 2.0 s and 2.0 to 3.0 s, respectively. These shapes show some of the first-order characteristics that are typical with this type of parachute opening. These include the initial ball of air filling the apex of the canopy and then inflating the canopy from apex to skirt. The model also predicts a phenomenon known as wake recontact. Wake recontact can occur in finite mass openings during or soon after the payload has undergone maximum deceleration. The wake trailing the opening canopy is moving close to the speed of the payload. As a result, when the payload undergoes its maximum deceleration, the wake contacts the apex of the canopy. The recontacting wake results in a negative differential pressure that indents the apex of the canopy. This phenomena can be seen in Fig. 4b.

The predicted payload position and velocity curves as functions of time are shown in Figs. 5 and 6, respectively. The payload reaches a maximum descent rate just prior to the first full opening of the parachute canopy. The payload then steadies out and approaches a terminal descent rate around 18 ft/s. Figure 7 plots the numerically predicted payload force vs time curve and two payload force vs time curves from the experiments. The force vs time curves are very close considering the approximations used in the model. The difference between the numerical and experimental results from the start of the simulation up to approximately 0.7 s is because of the representation of the initial shape of the canopy in the coupled model

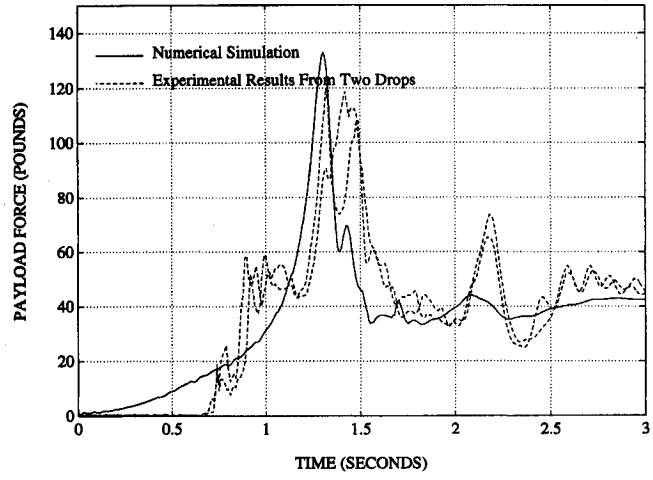


**Fig. 7 Payload force vs time (numerical and experimental).**

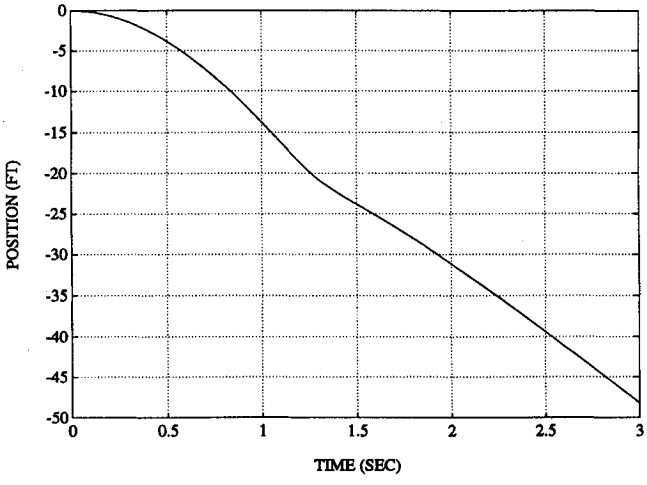


**Fig. 5 Payload position vs time.**

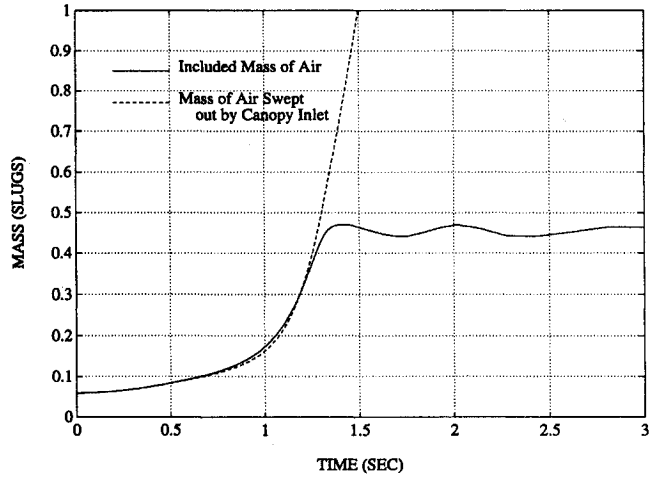


**Fig. 8 Included mass compared to swept out mass.**

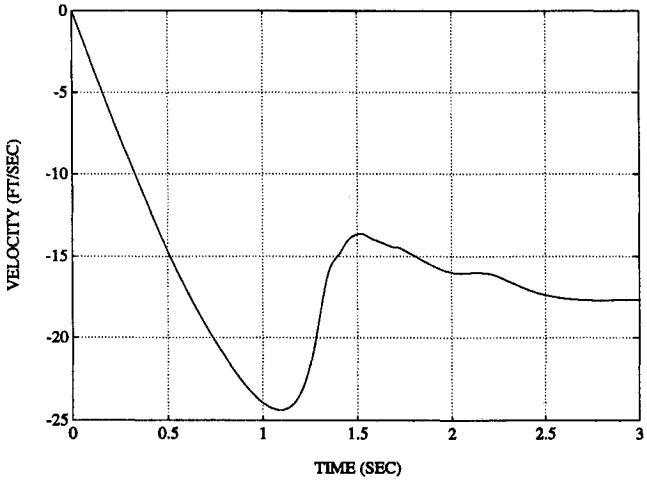


**Fig. 6 Payload velocity vs time.**

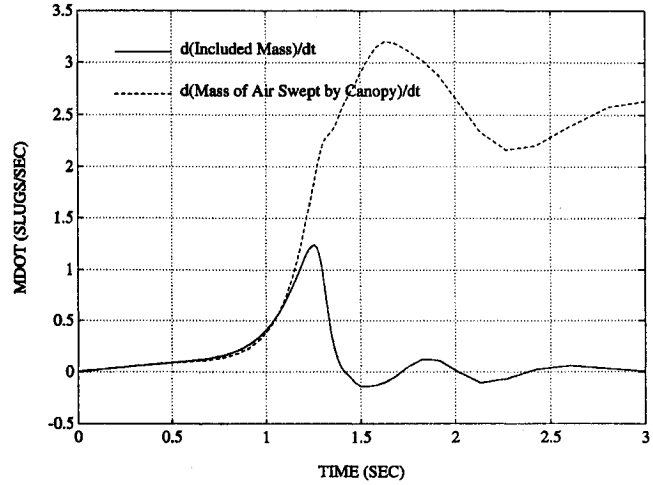


**Fig. 9 Time derivatives of included mass and swept out mass.**

that has a larger initial volume than the experimental canopies. The numerical curve predicts the approximate time and magnitude of the peak opening force and experiences a second peak force just after 2 s. The second peak in the force curve is because of a breathing of the parachute canopy that is observed in the experiments. Also note that the normal canopy damping input value has a strong effect on the peak force value. The larger the damping constant the lower the numerically predicted peak force. The numerical model does predict the time at which the peak opening force will occur.

The numerical model can also be used to investigate added mass effects during parachute opening. As an example, the included mass (defined as the mass of air confined to the interior volume contained by the parachute canopy) for incompressible flow can be calculated as the fluid density times the contained volume. Figure 8 shows the included mass vs time for the computation. Previous theories for parachute inflation have related the canopy filling time to the mass of air swept out by the canopy.[6] Figure 8 also shows this mass of air swept out by the canopy skirt that continues to grow in time. This

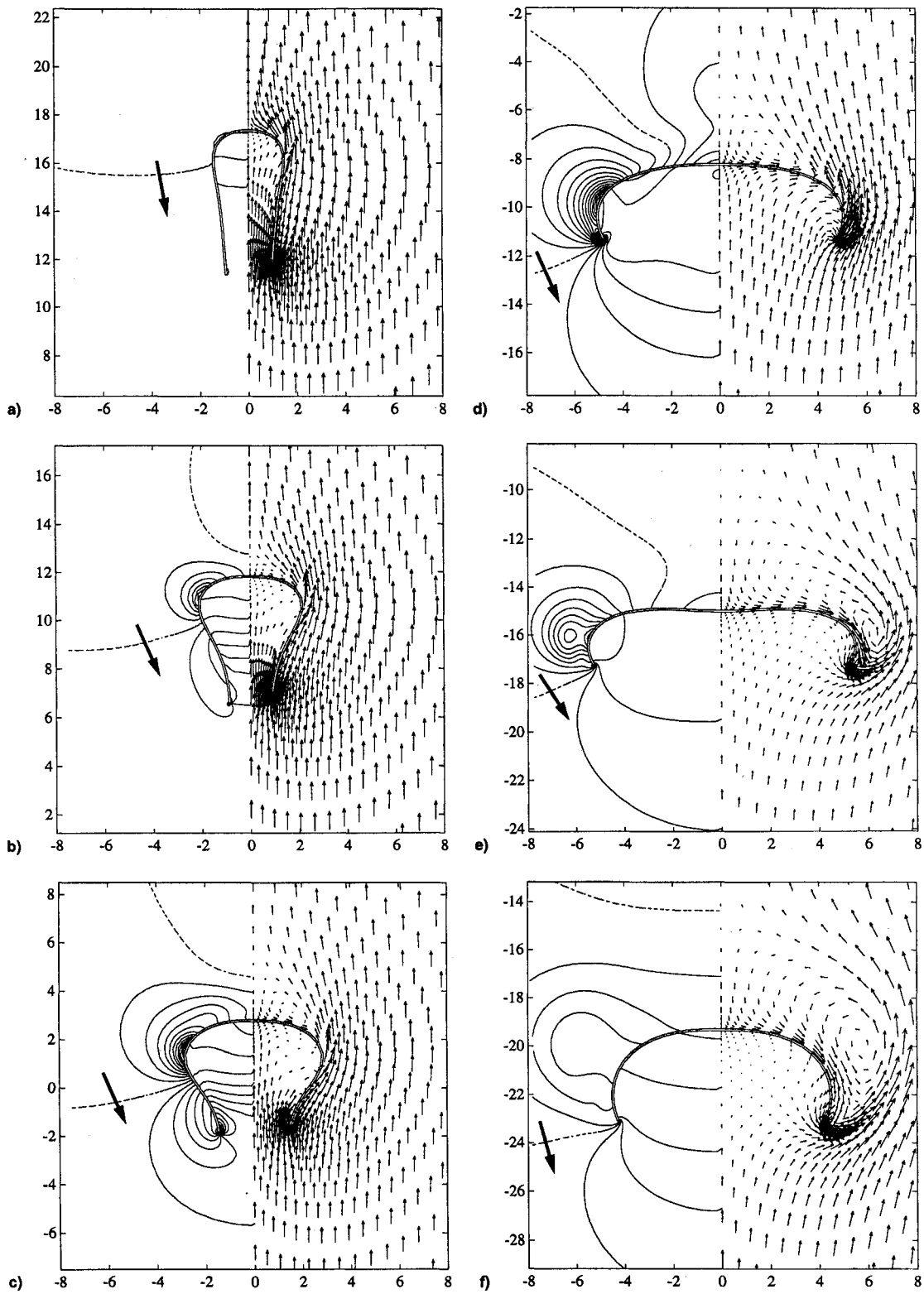


**Fig. 10 CFD pressure distributions and velocity vectors during opening: a) 0.4, b) 0.8, c) 1.2, d) 1.6, e) 2.0, and f) 2.4 s.**

mass is defined as the density of air times the volume that the parachute mouth encircles during descent. In reality, some air below the mouth escapes around the canopy as the canopy passes by. However, Fig. 8 indicates that during most of the opening the theory is acceptable, but after 1 s the two curves begin to diverge. Figure 9 shows the time derivatives of the curves shown in Fig. 8. As expected, the included mass approaches a constant value as the canopy reaches terminal descent, and therefore, the rate of change of the swept out mass approaches a nonzero value equal to the steady-state velocity times the steady-state skirt area times the density of air.

The pressure distributions and velocity vectors surrounding the canopy are shown in Figs. 10a–10f for six different time snapshots during the simulation. The pressure contour lines are shown on the left-hand side of each figure. The pressure range between contour lines in these figures is 0.1 psf. An arrow is drawn through the ambient pressure contour (dashed lines) indicating the direction of increasing pressure. The right-hand side of these figures shows the velocity vectors. The velocity vectors are scaled equally for each snapshot to provide information on the time-dependent velocity field in a consistent manner.

## Conclusions

The complexity of modeling the opening process stems from the coupling between the structural dynamics of the canopy, lines plus payload, and the aerodynamics of the surrounding fluid medium.

This article describes ongoing research at the U.S. Army Natick Research, Development, and Engineering Center, which involves the coupling of a CFD code and a structural dynamics code. The solution to the coupled problem is expected to assist in the development of future U.S. Army airdrop systems, which include the capability of deploying at low altitudes and high speeds. The capability of accurately predicting the behavior of parachute systems will significantly reduce the amount of testing currently required. Initial computational results with the model described in this article compare favorably with experimental data. However, the current model will require significant improvements and enhancements before it can be considered usable as a design aid. Future computational models are expected to provide significant insight about the behavior of parachutes during the opening process.

## References

[1]Stein, K. R., Benney, R. J., and Steeves, E. C., "A Computational Model that Couples Aerodynamic and Structural Dynamic Behavior of Parachutes During the Opening Process," NATICK/TR-93/029, April 1993.

[2]Stein, K. R., and Benney, R. J., "Parachute Inflation: A Problem in Aeroelasticity," NATICK/TR-94/015, Aug. 1994.

[3]Amsden, A. A., Ruppel, H. M., and Hirt, C. W., "SALE: A Simplified ALE Computer Program for Fluid Flow at All Speeds," Los Alamos National Lab. TR, LA-8095, 1980.

[4]Sundberg, W. D., "New Solution Method for Steady-State Canopy Structural Loads," *Journal of Aircraft*, Vol. 25, No. 11, 1988, pp. 1045–1051.

[5]"SLATEC Library, FORTRAN Mathematical Subprograms," National Energy Software Center.

[6]French, K. E., "Inflation of a Parachute," *AIAA Journal*, Vol. 1, No. 11, 1963, pp. 2615–2617.